Macromolecules **2005,** *38,* 1141−1147

Study of the Thermal Elimination and Degradation Processes of *n*-Alkylsulfinyl−PPV and −OC_1C_{10}−PPV Precursor Polymers with in Situ Spectroscopic Techniques

E. Kesters,[†] D. Vanderzande,[*,†,‡] L. Lutsen,[‡] H. Penxten,[†] and R. Carleer[†]

Division Chemistry, IMO, Limburgs Universitair Centrum, Universitaire Campus Bld. D,
B-3590 Diepenbeek, Belgium, and Division IMOMEC, IMEC, Universitaire Campus Bld. D,
B-3590 Diepenbeek, Belgium

Received March 6, 2004; Revised Manuscript Received November 5, 2004

ABSTRACT: We have studied the elimination reaction of *n*-alkylsulfinyl−PPV and −OC_1C_{10}−PPV precursor polymers toward conjugated materials with in situ FT-IR and UV−vis spectroscopy. The temperature at which the elimination reaction starts in nitrogen flow is as low as 65 and 70 °C, for the PPV and OC_1C_{10}−PPV precursor polymers, respectively. Under vacuum conditions, the elimination temperature shifts even to lower temperatures. After elimination, a certain amount of elimination products, which are set free during the elimination reaction, remain in the OC_1C_{10}−PPV polymer matrix, while in pure PPV, the elimination products are ejected more extremely from the polymer matrix. After completion of the elimination reaction, an absorption maximum of 416 and 490 nm ($T = 150$ °C) is obtained for the corresponding PPV and OC_1C_{10}−PPV, respectively. This effective conjugation length decreases again, by degradation of the conjugated system, around 330 °C for the PPV polymer and around 230 °C for the OC_1C_{10}−PPV polymer. From nonisothermal experiments in which the elimination reactions is studied in situ with FT-IR spectroscopy, we are able to determine an experimental activation energy (E_A) for the conversion reaction, which has a value that is in good agreement with the E_A that was obtained by theoretical modeling (104.6 kJ/mol or 25 kcal/mol).

Introduction

The microstructure of conjugated polymers is of major importance for their performance in the final applications; e.g., quality and morphology of the conjugated polymer strongly affects the performance of the material in polymeric light emitting devices (P-LED). In the case of precursor systems, both these properties may be strongly influenced by the elimination reaction. A large number of published papers deals with the conversion of sulfonium poly(*p*-phenylenevinylene) (PPV) precursor polymers.[1] The broad range of elimination conditions that are defined in these reports, however, underline the difficulty of monitoring the conversion reaction. For the sulfinyl−PPV precursor polymers the elimination was performed at 280 °C based on thermogravimetric analysis (TGA) analysis, because other tools for studying the elimination reaction were not available at that time.[2] Some years later, Margreet de Kok et al. investigated the elimination process in more detail by doing ex situ heating experiments.[3,4] A lot of questions, however, remained unanswered. In our view, this had the consequence that, to monitor the elimination reaction of sulfinyl−PPV precursor polymers toward conjugated polymers, the use of several complementary in situ analytical techniques is necessary.

With such in situ techniques, we are also able to study the degradation process of the conjugated PPV polymers. Within this context it should be noted that "apparent" stabilities up to 550 °C have been reported for plain PPV.[5] As we will show from in situ Fourier transform-infrared (FT-IR) and ultraviolet−visible (UV−vis) spectroscopy data, it is clear that at much lower temperatures chemical changes can occur, resulting in destruction of the conjugated chromophore.

Scheme 1. (I) Mechanism of the Elimination Reaction and (II) Dimerization and Disproportionation of Sulfenic Acids

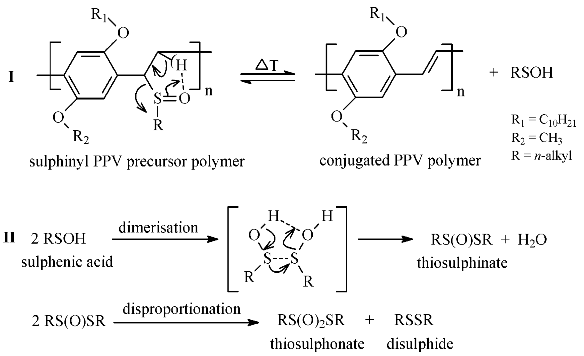

Concerning the elimination mechanism here under study, it is considered to take place via a syn-elimination (via a five-membered ring) in which the intermediate has a planar structure. This planar conformation can account in general for the selectivity to form trans double bonds: sterical hindrance between phenyl groups obstruct a cis double bond from being formed (Scheme 1, **I**). This process leads to the expulsion of sulfenic acids as the vinylic bond is formed.[6−8] The sulfenic acids which are split off are unstable and immediately dimerize to give thiosulfinates with concomitant loss of water.[9] The thiosulfinates disproportionate with the formation of thiosulfonates and disulfides (Scheme 1, **II**).[10−12] These products are called elimination products in this study.

The conjugated polymers that are studied here are poly(*p*-phenylenevinylene) (PPV) and poly[2-(3′,7′-di-

---

[*] Corresponding author. E-mail: dirk.vanderzande@luc.ac.be. Telephone: +32-11-268321. Fax: +32-11-268301.

[†] Limburgs Universitair Centrum.

[‡] IMEC.

10.1021/ma049545u CCC: $30.25

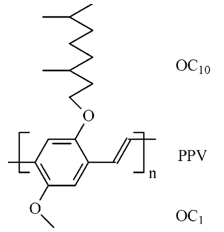

Figure 1. Structure of poly[2-(3′,7′-dimethyloctyloxy)-5-methoxy-1,4-phenylenevinylene (OC$_1$C$_{10}$−PPV).

methyloctyloxy)-5-methoxy-1,4-phenylenevinylene], or OC$_1$C$_{10}$−PPV. PPV itself can only be applied in electronic devices as a P-LED by use of a precursor route.[13,14] OC$_1$C$_{10}$−PPV on the other hand is a typical example of a material that is soluble in its conjugated form (Figure 1).[15−19] Over the past few years, much of the research emphasis was focused on the latter polymers, because of their relatively easy synthesis, their good processing capabilities into single-layer devices, and their high luminescence yields.[20] Recently promising results were also obtained for its use in photovoltaic cells (i.e., solar cells).[21−24] Therefore, OC$_1$C$_{10}$−PPV has become a standard electroluminescent material within the P-LED and plastic solar cell research.

The most used synthetic route to prepare the OC$_1$C$_{10}$−PPV conjugated polymer is the direct “Gilch route”, a one-step synthesis in a basic environment.[25] Another promising synthetic route to prepare the conjugated OC$_1$C$_{10}$−PPV polymer is a nonionic precursor route developed in our group, the “sulfinyl route”.[26−29] Note that because the OC$_1$C$_{10}$−PPV conjugated polymer is a soluble PPV derivative, the thermal elimination from a precursor polymer to the conjugated form can be carried out in solution as well as in the solid state.

In this paper an effort will be established to correlate the data of several in situ analytical techniques, such as TGA, direct insert probe mass spectrometry (DIP−MS), in situ FT-IR spectroscopy, and in situ UV−vis spectroscopy, to develop a clear picture of the elimination process and degradation behavior of the resulting conjugated polymer in solid state.

Experimental Section

Materials. The *n*-butyl− and *n*-octylsulfinyl−PPV monomers were synthesized and polymerized as described before.[30,31] The *n*-alkylsulfinyl−OC$_1$C$_{10}$−PPV monomers were also synthesized and polymerized as described before.[32]

Analytical Techniques. TGA measurements was performed on a TA instrument 951 thermogravimetric analyzer with a continuous nitrogen flow of 80 mL/min and a heating rate of 10 °C/min. Samples of precursor polymer (10 mg) were inserted in the solid state.

Direct insert probe mass spectroscopy (DIP−MS) analysis was carried out on a Finnigan TSQ 70, electron impact mode, mass range of 35−500. Electron energy was 70 eV. A CHCl$_3$ solution of precursor polymer was applied on the heating element of the direct insert probe. A similar heating rate of 10 °C/min was used to ensure a good comparison with TGA data.

The in situ elimination reactions were performed in a Harrick high-temperature cell (purchased from Safir), which was positioned in the beam of a Perkin-Elmer spectrum one FT-IR spectrometer (nominal resolution 4 cm^{-1}, summation of 16 scans). The temperature of the sample was controlled by a Watlow (serial number 999, dual channel) temperature controller. The precursor polymer was spin-coated from a CHCl$_3$ solution (6 mg/mL) on a KBr pellet at 500 rpm (film thickness approximately 400 nm-700 nm). The spin-coated KBr pellet (diameter 25 mm, thickness 1 mm) was in direct contact with the heating element. All experiments were performed at a heating rate of 2 °C/min. “Timebase software” supplied by Perkin-Elmer was used to investigate regions of interest.

In situ UV−vis measurements were performed on a Cary 500 UV−vis−NIR spectrophotometer, specially adapted by Varian to contain a Harrick high-temperature cell (scan rate 600 nm/min, continuous run from 200 to 600 nm). The precursor polymers were spin-coated from a CHCl$_3$ solution (6 mg/mL) on a quartz glass (diameter 25 mm, thickness 3 mm) at 700 rpm (film thickness approximately 100 nm-400 nm). The quartz glass was heated in a Harrick high temperature cell specially adapted by Harrick to be positioned in the beam of the UV−vis−NIR-spectrophotometer. Spectra were taken continuously. The heating rate was 2 °C/min up to 300 °C. Reproducibility is within a range of 5% relative to the temperatures depicted and relates to the homogeneity of the film deposited.

All measurements were performed under a continuous flow of nitrogen. “Scanning Kinetics software” supplied by Varian was used to investigate regions of interest. To be sure that no changes occurred at certain wavelengths due to the quartz disk itself, an in situ UV−vis nonisothermal heating experiment from ambient temperature up to 250 °C was performed on a blanco quartz disk. The absorbance of the most common wavelengths studied during the elimination and degradation process remained unchanged during the experiment. This means that the quartz disk itself had no influence on the absorbance at these wavelengths during the elimination and degradation process from precursor polymer toward conjugated polymer.

Results and Discussion

Thermal Analysis: TGA and DIP—MS. In first instance, two classical techniques were used to study the thermal stability of the precursor polymers. The first technique is thermogravimetric analysis (TGA), while the second technique is direct insert probe mass spectroscopy (DIP−MS). In TGA, the weight loss is recorded as a function of temperature. The conversion from a *n*-alkylsulfinyl−PPV or −OC$_1$C$_{10}$−PPV precursor polymer to a conjugated polymer can easily be monitored with TGA, because the conversion reaction is accompanied by weight loss due to evaporation of the elimination products. For each precursor polymer, weight loss is observed in three temperature regions. First, a relatively small loss of weight is observed just below 100 °C, which is assigned to evaporation of water, present on the hygroscopic sulfinyl groups.[33] Above 100 °C, two major steps of weight loss are visible, the first step is related to the elimination of the S-groups itself and to the evaporation of the elimination products that are liberated during the elimination process. The second major weight loss accounts for the degradation of the conjugated polymer. Those elimination, evaporation, and degradation temperatures are summarized in Table 1.

A second important technique we use in the study of the thermal stability of *n*-alkylsulfinyl−PPV polymers and to get information about the structure of the elimination products, is thermal analysis by direct insert probe mass spectroscopy (DIP−MS). The total reconstructed ionchromatogram, in which the total ion current (TIC) is plotted vs increasing temperature, shows two signals. The fragments observed in the mass spectrum of the first peak are consistent with dimerization and disproportionation processes of sulfenic acids, thus the elimination itself. The second signal in the ionchromatogram is related to the degradation of the conjugated polymer. Elimination and degradation temperatures obtained from DIP−MS are summarized in Table 1.

Table 1. Elimination, Evaporation, and Degradation Temperatures Obtained from TGA and DIP−MS Analysis for the *n*-Alkylsulfinyl−PPV and OC_1C_{10}−PPV Polymers

	TGA			DIP−MS	
	elimination max (°C)	elimination−evaporation (°C)	degradation max (°C)	elimination max (°C)	degradation max (°C)
n-butyl−S(O)−PPV	146	100−250	546	131	501
n-octyl−S(O)−PPV	256	100−300	549	134	502
n-ethyl−S(O)−OC_1C_{10}−PPV	151	115−230	423	132	358
n-butyl−S(O)−OC_1C_{10}−PPV	155	120−348	423.1	135	301
n-octyl−S(O)−OC_1C_{10}−PPV	162	110−353	425.6	145	297

The difference between TGA and DIP−MS analysis is the atmosphere in which the experiment is carried out. TGA is performed in argon atmosphere, whereas DIP−MS experiments are executed in high vacuum conditions (10^{-6} mmHg). The high vacuum in the mass spectrometer causes a weight loss and a corresponding ion current at lower temperatures, because the evaporation is faster compared with a heating process in argon atmosphere (TGA). In DIP−MS, an apparent lower thermal stability can be derived for most functionalities. Comparison of the DIP−MS observations with the TGA data indicates that under argon flow the elimination reaction and evaporation of the elimination products are kinetically separated, more so for the *n*-octyl derivative than for the *n*-ethyl and *n*-butyl derivatives. *n*-Octyl elimination products have higher boiling points than *n*-ethyl and *n*-butyl elimination products, which means that their evaporation out of the polymer matrix is delayed. Consequently, evaporation and elimination are no longer separated in the high vacuum conditions in DIP−MS.[34] Hence the elimination temperature retrieved from DIP−MS is more realistic than that obtained from TGA. Still even the former measurements only allow a relative indirect observation of the elimination and degradation processes.

Study of the Elimination and Degradation Reaction of *n*-Alkylsulfinyl—PPV and OC_1C_{10}—PPV Precursor Polymers with in Situ FT-IR Spectroscopy. To obtain more detailed information about the temperature range in which the elimination and degradation reaction take place, an in situ nonisothermal heating experiment was performed with the *n*-alkylsulfinyl−PPV and −OC_1C_{10}−PPV precursor polymers at 2 °C/min from ambient temperature up to 450 and 350 °C respectively, under a continuous flow of nitrogen. Before heating, at 25 °C, the *n*-alkylsulfinyl−OC_1C_{10}−PPV precursor polymer is a yellow sticky solid product which turns red after the elimination reaction. The *n*-alkylsulfinyl−PPV precursor polymer is a white solid product, which turns yellow during the elimination reaction. At much higher temperatures, the red (OC_1C_{10}−PPV) and yellow (PPV) colors change to black due to degradation of the conjugated polymer. The elimination from precursor to conjugated polymer can be followed via the formation of the *trans*-vinylene double bond (965 cm^{-1}) as well as by the disappearance of the IR absorbances of the sulfinyl group (1038 (*n*-butyl)/1046 cm^{-1} (*n*-octyl)) and the CH_2 asymmetrical stretch (2925 cm^{-1}) vs temperature. The degradation of the conjugated polymer can be followed by the disappearance of the trans vinylene double bond at 965 cm^{-1} vs temperature. This is shown in Figure 2, parts A and 2B for the PPV and OC_1C_{10}−PPV precursor polymer, respectively.

From Figure 2A, it is clear that the elimination for the *n*-butylsulfinyl−PPV precursor polymer in these conditions starts already at 65 °C. The IR absorbances of the sulfinyl group at 1038 cm^{-1} and the alkyl group at 2925 cm^{-1} have no detectable absorption anymore after elimination at 120 °C. In the region between 120 and 330 °C, there is a slight decrease in the absorbance of the double bond. This is not due to decomposition of the PPV material, but it is related to a thermochromic effect as was demonstrated by successive heat−cool cycles (see further). The thermochromic effect in conjugated polymers is here defined as the reversible change of the absorption maximum as a consequence of an increase or decrease of the average torsion angle in the conjugated system and thus “effective conjugation length”, under the influence of a change in temperature. At temperatures around 330 °C (fast decrease in the absorbance at 965 cm^{-1}), degradation of the conjugated system occurs. This degradation temperature observed with in situ FT-IR spectroscopy is much lower than the one obtained with TGA and DIP−MS. Therefore, one

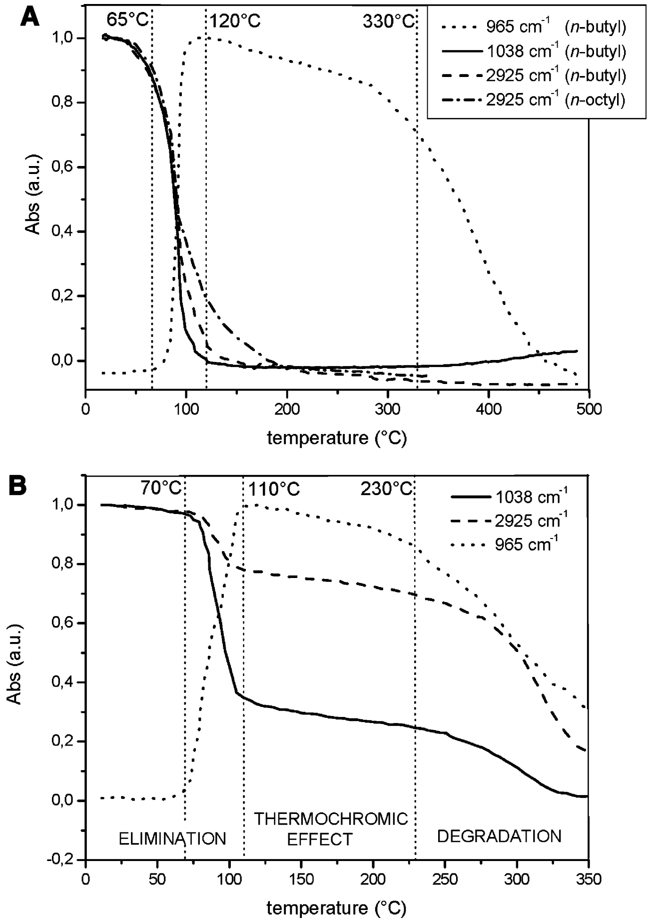

Figure 2. A. Absorbance at 1038, 965, and 2925 cm^{-1} as a function of increasing temperature for the *n*-alkylsulfinyl−PPV precursor polymer. B. Absorbance at 1038, 965, and 2925 cm^{-1} as a function of increasing temperature for the *n*-butylsulfinyl−OC_1C_{10}−PPV precursor polymer.

should be careful with using the conversion temperatures reported in the literature to obtain pure PPV. For conversion of a precursor, elimination temperatures of 250 °C for several hours are often used, but 250 °C is far too high and lies very close to the starting temperature of degradation of the conjugated PPV structure. Identical results in elimination and degradation behavior are obtained with the *n*-octylsulfinyl as eliminable group, but as can be clearly observed in Figure 2A, the absorbance at 2925 cm^{-1} decreases much slower compared to the absorbance of the sulfinyl group. This means that it is more difficult for the *n*-octyl elimination products to evaporate out of the polymer matrix, while the elimination reaction is already complete at 120 °C (the same temperature as for the *n*-butyl derivative). These results confirm the interpretation of the results obtained from comparison of the TGA and DIP−MS data.

From Figure 2B, it is obvious that the elimination for the *n*-butylsulfinyl−OC_1C_{10}−PPV precursor polymer starts at approximately 70 °C and is completed when approximately 110 °C is reached. Again the absorbances at 965, 1038, and 2925 cm^{-1} can be used to monitor the formation of the double bond, evaporation of the elimination products and stability of the polymer. The elimination reaction for the *n*-alkylsulfinyl−OC_1C_{10}−PPV precursor polymers occurs almost in the same temperature region as that for the *n*-alkylsulfinyl−PPV precursor polymers (Figure 2A). Between 110 and 230 °C, there is a slight decrease in the absorbance of the double bond. This is related to a thermochromic effect, as mentioned before. At temperatures around 230 °C (fast decrease in the absorbance at 965 cm^{-1}), degradation of the conjugated system seems to occur. As soon as the conjugated polymer backbone begins to degrade, the absorbance of the CH_2 asymmetrical stretch at 2925 cm^{-1} decreases further. This means that as the degradation of the conjugated system occurs, also the alkoxy chain (OC_{10}) or part of the alkoxy chain is split off from the polymer backbone.

From Figure 2B, it is also clear that ~ 30% of the sulfinyl absorbance is still present in the polymer film after elimination at 110 °C. This was not the case after the thermal elimination of the *n*-alkylsulfinyl−PPV precursor polymers, without alkoxy chains on the polymer backbone (Figure 2A). The source of this interference are the thiosulfinates and thiosulfonates which contain a S(O) and $S(O)_2$ group respectively and are formed during the elimination reaction.[35] These elimination products may be soluble in the OC_1C_{10}−PPV polymer matrix. The decane chain (from OC_{10}), which is covalently bonded with the polymer backbone, acts then as the solvent. As a result, the elimination products are expected to be homogeneously distributed within the OC_1C_{10}−PPV polymer matrix. In the case of pure PPV, the elimination products and the polymer matrix are incompatible leading very probably to phase separation and thus in pure PPV, the elimination products are ejected more extremely from the polymer matrix. This points to a serious problem, as these elimination products, being very sensitive at high temperatures, could attack the conjugated polymer. Therefore, it is better to do the elimination reactions with a precursor polymer that has a sulfinyl eliminable group with a small alkyl chain, because the smaller the alkyl chain, the lower the boiling point of the corresponding elimination products, the easier the elimination products will evaporate or diffuse out of the polymer matrix. A second solution for this problem is to do the same thermal elimination reaction, but now under vacuum conditions instead of nitrogen flow, to increase the volatility of the elimination products. In these experiments we observed that under vacuum conditions, the elimination reaction starts at 53 °C instead of 70 °C for each *n*-alkylsulfinyl−OC_1C_{10}−PPV polymer, which is earlier compared to the elimination reaction under nitrogen flow. The fact that the starting temperature of the elimination reaction is lower in a vacuum conditions than in nitrogen flow, demonstrates that an equilibrium condition is present, which can be shifted through promoting the evaporation.

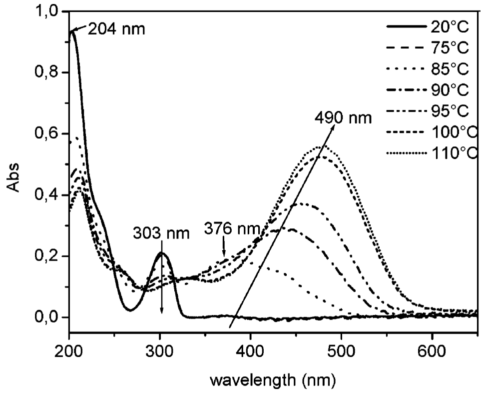

Figure 3. UV-absorption spectra of the *n*-butylsulfinyl−OC_1C_{10}−PPV precursor polymer at different temperatures.

Study of the Elimination and Degradation Reaction of *n*-Alkylsulfinyl—PPV and —OC_1C_{10}—PPV Precursor Polymers with in Situ UV—Vis Spectroscopy. To complete the study concerning the elimination and degradation reaction of PPV and OC_1C_{10}−PPV polymers, obtained from in situ FT-IR spectroscopy, a procedure similar to that for FT-IR is used in UV−vis. It is well-known that the absorption maximum of a conjugated polymer is displaced to higher wavelengths when the number of conjugated double bonds increases.[36,37] The UV-absorption is due to $\pi-\pi^*$ transition in the conjugated backbone and depends on the "effective conjugation length".[38] Figure 3 displays the UV-absorption spectra of an OC_1C_{10}−PPV polymer in film (on quartz disk) at different temperatures, during the thermal elimination process.

The broad absorption band of the conjugated π-electron system between 350 and 600 nm increases in intensity and shows a bathochromic shift with increasing temperatures. The broad low energy absorption is completed at 110 °C as the absorption edge shows no further red shifts (=saturation). The final red OC_1C_{10}−PPV polymer film, shows an absorption maximum (=λ_{max}) of 490 nm at 110 °C. The spectrum of the yellow conjugated PPV polymer film, at 120 °C, shows an absorption maximum at 416 nm (not shown here). Absorptions at 204 and 303 nm diminish progressively as the temperature increases.

It should also be noted that UV−visible light absorption becomes insensitive to increasing conjugation when the conjugation lengths exceed about eight repeating units.[39] As a result, this method cannot be used as a quantitative technique for conjugated polymers with high degrees of elimination.

In Figure 4, the change in λ_{max} for the OC_1C_{10}−PPV is depicted as a function of temperature. Between 50 and 75 °C, small conjugated segments (oligomers) are

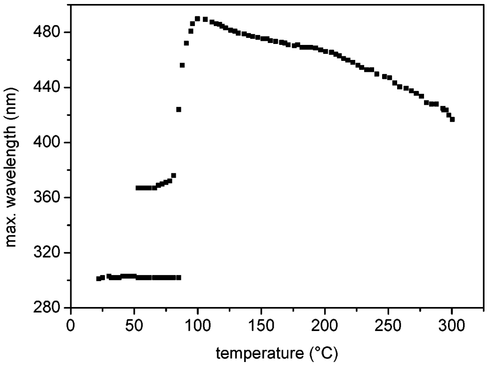

Figure 4. Wavelength at maximum absorption (nm) as a function of increasing temperature for the *n*-butylsulfinyl−OC_1C_{10}−PPV precursor polymer.

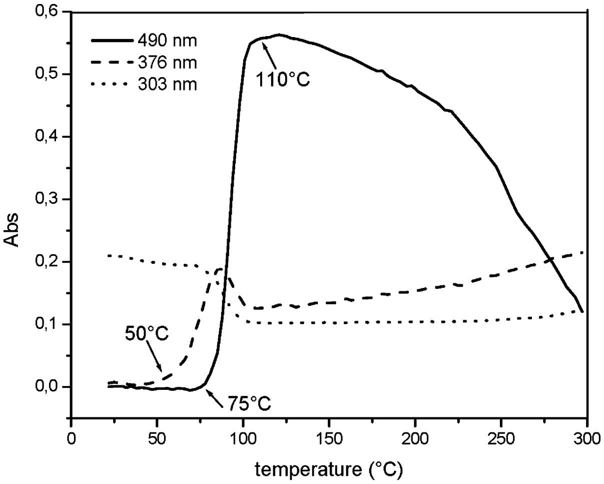

Figure 5. Absorbance at 303, 376, and 490 nm as a function of increasing temperature for the *n*-butylsulfinyl−OC_1C_{10}−PPV precursor polymer.

formed. In this temperature range a shift in maximum absorption is visible from 302 nm until 376 nm. Between 80 and 110 °C, a transition from oligomer fragments to longer conjugated segments occurs, which finally reaches a λ_{max} of 490 nm at 110 °C. From 110 until 230 °C, this λ_{max} gradually shifts from 490 nm until 454 nm, due to a thermochromic effect. Between 230 and 300 °C, degradation occurs, the λ_{max} shifts further to shorter wavelengths (416 nm) (hypsochromic shift), due to the loss of conjugation upon degradation.

The same tendencies are visible in Figure 5, in which we have plotted the absorbance of three specific absorption maximum (303, 376, and 490 nm corresponding with the precursor polymer, oligomeric fragments and the conjugated system respectively) as a function of increasing temperature. The increase in the absorbance at 376 nm indicates that the oligomeric fragments are formed between 50 and 75 °C. As the elimination proceeds, between 75 and 110 °C, the absorbance at 376 and 303 nm decreases and the absorbance at 490 nm increases. At temperatures higher than 110 °C, the absorbance at 376 nm increases while the absorbance at 490 nm decreases again. This means that shorter conjugation lengths are formed at the cost of the higher conjugation lengths. Two phenomena can explain this observation, a thermochromic effect on one hand and a degradation process of the conjugated polymer on the other hand. Both phenomena lead to a reduction of the effective conjugation length, visible as an increase in the absorbance at 376 nm. The striking similarity with the results obtained with FT-IR clearly demonstrates that both techniques are complementary.

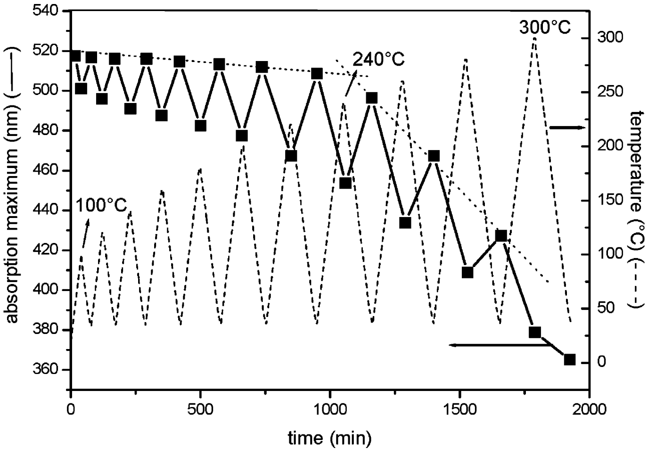

Figure 6. Temperature−time profile and the absorption maximum for the conjugated OC_1C_{10}−PPV polymer.

Table 2. λ_{max} at Each Maximum and Minimum in the Temperature Profile,Where the λ_{Max} of OC_1C_{10}−PPV at Ambient Temperature Is 517 nm

temp (°C)	λ_{max} (nm) at maximum temp	λ_{max} (nm) at 35 °C after cooling
100	501	517
120	496	516
140	491	516
160	487.5	515
180	482.5	513
200	477.5	512
220	467.5	509
240	453.7	496.5
260	433.7	467.5
280	408.7	427.2
300	378.5	365

During the nonisothermal experiment, we have noticed that between 110 and 230 °C, for the OC_1C_{10}−PPV polymer, the absorbance at 490 nm (UV−vis) and at 965 cm^{-1} (FT-IR) is slightly decreasing. These observations may be caused by a “thermochromic effect” as was mentioned before. By heating of the conjugated polymer, the mobility of the polymer chains increases, which implies an increase of the average torsion angle and thus the binding energy becomes smaller. The effective conjugation length decreases, which reflects in a blue shift. This process should be reversible.

To prove that degradation of the conjugated OC_1C_{10}−PPV polymer starts only around 230 °C, a heating−cooling experiment is performed on the already conjugated OC_1C_{10}−PPV polymer. This red OC_1C_{10}−PPV polymer is eliminated in solution (toluene, 110 °C for 4 h), precipitated in methanol and collected and dried in a vacuum. This conjugated OC_1C_{10}−PPV polymer is then heated at 2 °C/min up to different temperatures and is cooled again to 35 °C each time, under a continuous flow of nitrogen. In Figure 6, this time−temperature profile is depicted. Also, the absorption maximum (λ_{max}) at each maximum (100, ..., 240, ..., 300 °C) and minimum (35 °C) in the temperature profile are displayed. The UV data results are summarized in Table 2.

The absorption maximum (λ_{max}) of the conjugated OC_1C_{10}−PPV polymer eliminated in solution and measured in film at ambient temperature is 517 nm. By heating of the conjugated OC_1C_{10}−PPV polymer, the effective conjugation length decreases. For instance,

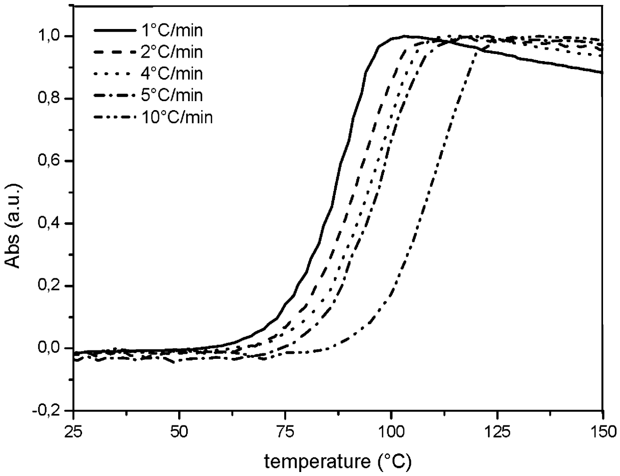

Figure 7. Absorbance of the trans double bond at 965 cm^{-1} as a function of temperature at different heating rates for the n-butylsulfinyl$-OC_1C_{10}-$PPV precursor polymer.

when the conjugated $OC_1C_{10}-$PPV polymer is heated to 100 °C, the λ_{max} is shifted from 517 to 501 nm. After cooling the conjugated $OC_1C_{10}-$PPV polymer again, the conjugated system is fully recovered and a λ_{max} of 517 nm is observed again. This "thermochromic effect" can be repeated for higher temperatures. Up to ~ 220 °C, the original λ_{max} is recovered after cooling. From 240 °C on, however, and after the sample is allowed to cool back to ambient temperature, a clear blue shift (λ_{max} = 496.5 nm) is visible compared with the λ_{max} of the conjugated $OC_1C_{10}-$PPV polymer at ambient temperature (λ_{max} = 517 nm). This blue shift becomes larger at temperatures >240 °C. The process now is not reversible anymore, meaning that degradation of the conjugated system itself has occurred. The results discussed here are consistent with the results obtained from Figures 2B and 5. Consequently, the small decrease in the absorbance at 490 nm and 965 cm^{-1} between 110 and 230 °C is thus due to a thermochromic effect, while the fast decrease in the absorbance at 490 nm and 965 cm^{-1}, at temperatures >230 °C, is due to degradation of the conjugated $OC_1C_{10}-$PPV polymer.

The Effect of Heating Rate under Nonisothermal Conditions: Kinetic Analysis of Derivative Curves in Thermal Analysis, Studied with in Situ FT-IR Spectroscopy. Knowledge of kinetic parameters, such as the reaction rate and activation energy, offers the opportunity to determine the reaction mechanism in solid phases. For nonisothermal heating experiments these kinetic parameters could be obtained by the method of Ozawa. The "method of Ozawa" is a nonisothermal isoconventional kinetic method and is independent of the reaction model (=model-free methodology).[40,41] This model-free methodology allows us to determine the dependence of the activation energy on the extent of conversion.

The n-octylsulfinyl$-OC_1C_{10}-$PPV precursor polymer is heated from ambient temperature up to 150 °C at different heating rates (1, 2, 4, 5, and 10 °C), under a continuous flow of nitrogen. For the method of Ozawa and to determine the temperature range in which the elimination reaction takes place, the absorbance of the trans vinylene double bond at 965 cm^{-1} is followed during the conversion process as a function of temperature at different heating rates and is shown in Figure 7. When the heating rate is increased, the absorbance at 965 cm^{-1} shifts to higher temperatures. The method of Ozawa uses this shift to calculate the activation energy of the conversion reaction. The first derivative of these curves to the temperature, shows a maximum at a certain temperature T_m, which is dependent on the heating rate β (Figure 8).

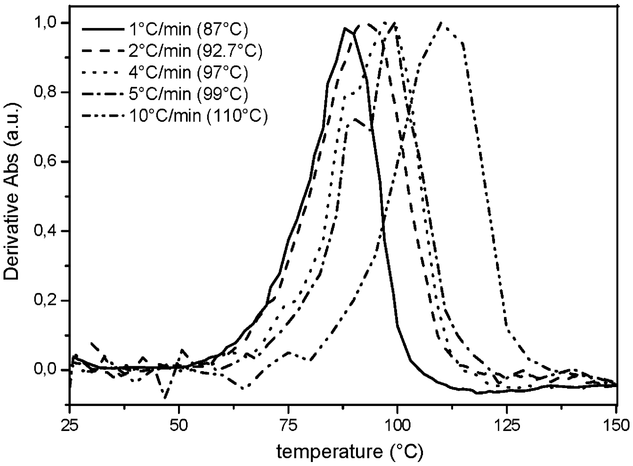

Figure 8. First derivative of the absorbance of the trans double bond at 965 cm^{-1} at different heating rates.

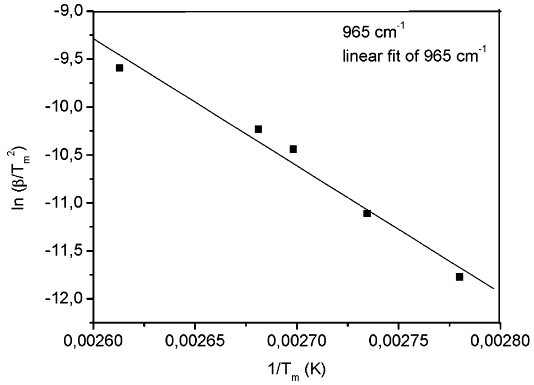

Figure 9. Ozawa plot for the trans double bond (965 cm^{-1}) absorbance.

The heating rate β and the temperature T_m, for at least three measurements, permits one to determine the activation energy of the conversion reaction, eq 1.[40,41]

$$\ln\left(\frac{\beta}{T_m^{\,2}}\right) = -\frac{E_A}{RT_m} + \ln\left(\frac{AR}{E_A}\right) - \ln(g(\alpha)) \tag{1}$$

When $\ln(\beta/T_m^2)$ is plotted as a function of T_m^{-1}, for the trans double bond absorbance, a straight line with as slope $-E_A/R$ is obtained (Figure 9). From this, the activation energy can then be calculated ($E_A = -R \times$ slope).

The activation energy (E_A) for the conversion process, calculated from the experimental data of the trans vinylene double bond absorbance at 965 cm^{-1} is 110,3 kJ/mol (26.4 kcal/mol). From theoretical calculations on a sulfinyl precursor, an E_A of 104.6 kJ/mol (25 kcal/mol) is obtained for the conversion reaction to *trans*-stilbene,[42] this is in good agreement with our experimental results. However, nonisothermal measurements yield a valuation for the activation energy of the conversion reaction, but isothermal experiments are essential to realize a reliable determination. Studies involving such experiments are in progress.

Conclusions

We have demonstrated that the elimination reaction of the sulfinyl functionality in the PPV and OC_1C_{10}–PPV precursor polymers starts at relatively low temperatures, 65 and 70 °C, respectively. The degradation for both conjugated polymers occurs already at 330 and 230 °C, which is much lower compared to literature data. A value for the activation energy of the conversion reaction from an *n*-octylsulfinyl–OC_1C_{10}–PPV precursor polymer to the conjugated OC_1C_{10}–PPV polymer was determined using nonisothermal FT-IR measurements and is in good agreement with theoretical studies. A "thermochromic" effect was identified for the conjugated polymer, which occurs until the polymer degrades at said temperatures.

Acknowledgment. IWT is acknowledged for the Ph.D. grant for E.K., and Fonds voor Wetenschappelijk Onderzoek (FWO), BOF-LUC, and EFRO are acknowledged for financial support.

References and Notes

(1) Wessling, R. A. *J. Polym. Sci., Polym. Symp.* **1985**, *72*, 55.
(2) Louwet, F. Ph.D. Thesis. Limburgs Universitair Centrum, Diepenbeek, Belgium, 1993.
(3) de Kok, M. Ph. D Thesis. Limburgs Universitair Centrum, Diepenbeek, Belgium, 1999.
(4) de Kok, M. M.; van Breemen, A. J. J. M.; Carleer, R. A. A.; Adriaenssens, P. J.; Gelan, J. M.; Vanderzande, D. J. *Acta Polym.* **1999**, *50*, 28.
(5) Montaudo, G.; Vitalini, D.; Lenz, R. W. *Polymer* **1987**, *28*, 837–842.
(6) Kingsburry, C. A.; Cram, D. J. *J. Am. Chem. Soc.* **1960**, *82*, 1810.
(7) Shelton, J. R.; Davis, K. E. *Int. J. Sulfur Chem.* **1973**, *8*, 205.
(8) Yoshimura, T.; Tsukurimichi, E.; Iizuka, Y.; Mizuno, H.; Isaji, H.; Shimasaki, C. *Bull. Chem. Soc. Jpn.* **1989**, *62*, 1891.
(9) Trost, B. M.; Leung, K. K. *Tetrahedron Lett.* **1975**, *48*, 4197.
(10) Koch, P.; Ciuffarin, E.; Fava, A. *J. Am. Chem. Soc.* **1970**, *92*, 5971.
(11) Kice, J. L.; Cleveland, J. P. *J. Am. Chem. Soc.* **1973**, *95*, 109.
(12) Davis, F. A.; Jenkins, J. A.; Billmers, R. L. *J. Org. Chem.* **1986**, *51*, 1033.
(13) Burn, P. L.; Bradley, D. D. C.; Friend, R. H.; Halliday, D. A.; Holmes, A. B.; Jackson, R. W.; Kraft, A. *J. Chem. Soc., Perkin Trans* **1992**, *1*, 3225.
(14) Hsieh, B. R.; Antoniadis, H.; Bland, D. C.; Feld, W. A. *Adv. Mater.* **1995**, *7*, 36.
(15) Braun, D.; Heeger, A. J. *Appl. Phys. Lett.* **1991**, *58*, 1982.
(16) Staring, E. G. J.; Demandt, R. C. J. E.; Braun, D.; Rikken, G. L. J.; Kessner, Y. A. R. R.; Venhuizen, T. H. J.; Wynberg, H.; ten Hoeve, W.; Spoelstra, K. J. *Adv. Mater.***1994**, *6*, 934.
(17) Lee, J. K.; Schrock, R. R.; Baigent, D. R.; Friend, R. H. *Macromolecules* **1995**, *28*, 1966.
(18) Hilberer, A.; Brouwer, H. J.; van der Scheer, B. J.; Wildeman, J.; Hadziioannou, G. *Macromolecules* **1995**, *28*, 4525.
(19) Kim, D. U.; Tsutsui, T.; Saito, S. *Chem. Lett.* **1995**, 587.
(20) Kim, S. T.; Hwang, D. H.; Li, X. C.; Grüner, J.; Friend, R. H.; Holmes, A. B.; Shim, H. K. *Adv. Mater.* **1996**, 979.
(21) Gerlinck, G. H.; Warman, J. M.; Staring, E. G. J. *J. Phys. Chem.* **1996**, *100*, 5485.
(22) Brabec, C. J.; Sariciftci, N. S.; Hummelen, J. C. *Adv. Funct. Mater.* **2001**, *11* (1), 15.
(23) van der Ent, L. *Kunststof. Mag.* **2001**, Apr 3, 38.
(24) Munters, T.; Martens, T.; Goris, L.; Vrindts, V.; Manca, J.; Lutsen, L.; De Ceuninck, W.; Vanderzande, D.; De Schepper, L.; Gelan, J.; Saricifci, N. S.; Brabec, C. J. *Thin Solid Films* **2002**, *403*, 247.
(25) Gilch, H. G.; Wheelwright, W. L. *J. Polym. Sci., Part A: Polym. Chem.* **1966**, *4*, 1337.
(26) Louwet, F.; Vanderzande, D.; Gelan, J. *Synth. Met.* **1992**, *52*, 125.
(27) Louwet, F.; Vanderzande, D.; Gelan, J.; Mullens, J. *Macromolecules* **1995**, *28*, 1330.
(28) Louwet, F.; Vanderzande, D.; Gelan, J. *Synth. Met.* **1995**, *69*, 509.
(29) Issaris, A.; Vanderzande, D.; Gelan, J. *Polymer* **1995**, *38*, 2571.
(30) van Breemen, A. J. J. M.; Adriaensens, P. J.; Issaris, A. C. J.; de Kok, M. M.; Vanderzande, D. J. M.; Gelan, J. M. J. V. *Magn. Reson. Chem.* **2000**, *38*, 129.
(31) van Breemen, A. J. J. M.; de Kok, M. M.; Adriaensens, P. J.; Vanderzande, D. J. M.; Gelan, J. M. J. V. *Macrom. Chem. Phys.* **2001**, *202*, 343.
(32) Lutsen, L.; van Breemen, A. J.; Kreuder, W.; Vanderzande, D. J. M.; Gelan, J. M. J. V. *Helv. Chim. Acta* **2000**, *83*, 3113.
(33) Herold, M.; Gmeiner, J.; Schwoerer, M. *Acta Polym.* **1994**, *45*, 392.
(34) Kesters, E.; Lutsen, E.; Vanderzande, D.; Gelan, J. *Synth. Met.* **2001**, *119*, 311.
(35) Cymerman, J.; Willis, J. B. *J. Chem. Soc., London* **1951**, 1332.
(36) Sondheimer, F.; Efraim, D. A.; Wolousky, R. *J. Am. Chem. Soc.* **1961**, *83*, 1675.
(37) Daniels, V.; Rees, N. H. *J. Polym. Sci., Polym. Chem. Ed.* **1974**, *12*, 2115.
(38) Burn, P. L.; Kraft, A.; Baigent, D. R.; Bradley, D. D. C.; Brown, A. K.; Friend, R. H.; Gymer, R. W.; Holmes, A. B.; Jackson, R. W. *J. Am. Chem. Soc.* **1993**, *115*, 5, 10117.
(39) Drefahl, G.; Kuhmstedt, R.; Oswald, H.; Hoerhold, H. H. *Makromol. Chemie* **1970**, *131*, 89.
(40) Ozawa, T. *J. Therm. Anal.* **1970**, *2*, 301.
(41) Celis, K.; Van Driessche, I.; Mouton, R.; Vanhoyland, G.; Hoste, S. *Key Eng. Mater.* **2002**, *206*, 807.
(42) Claes, L.; Francois, J. P.; Deleuze, M. S. *J. Am. Chem. Soc.* **2002**, *124*, 7563.

MA049545U